Electronic Supplementary Information (ESI)

Aluminum Alkoxide, Amide and Halide Complexes Supported by a Bulky Dipyrromethene Ligand: Synthesis, Characterization, and Preliminary ε-Caprolactone Polymerization Activity

Christopher G. Gianopoulos†, Nishant Kumar‡, Yihong Zhao‡, Li Jia‡, Kristin Kirschbaum†, and Mark R. Mason†*

†Department of Chemistry, School of Green Chemistry and Engineering, The University of Toledo, Toledo, Ohio 43606-3390

‡ Department of Polymer Science, The University of Akron, Akron, Ohio 44325-3909

Table of Contents

Figures:

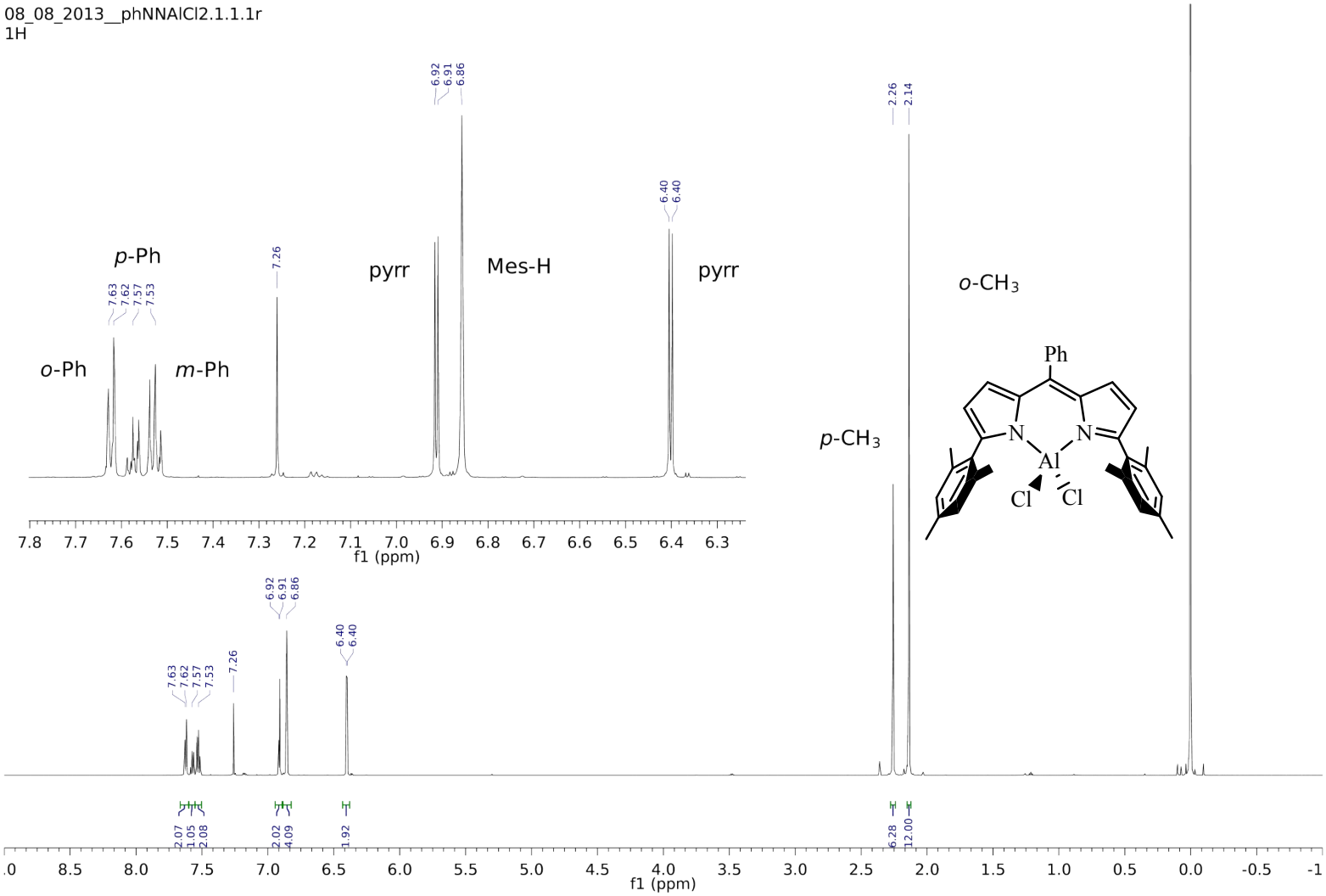

Figure S1. ^{1}H NMR spectrum of **2** in $CDCl_3$

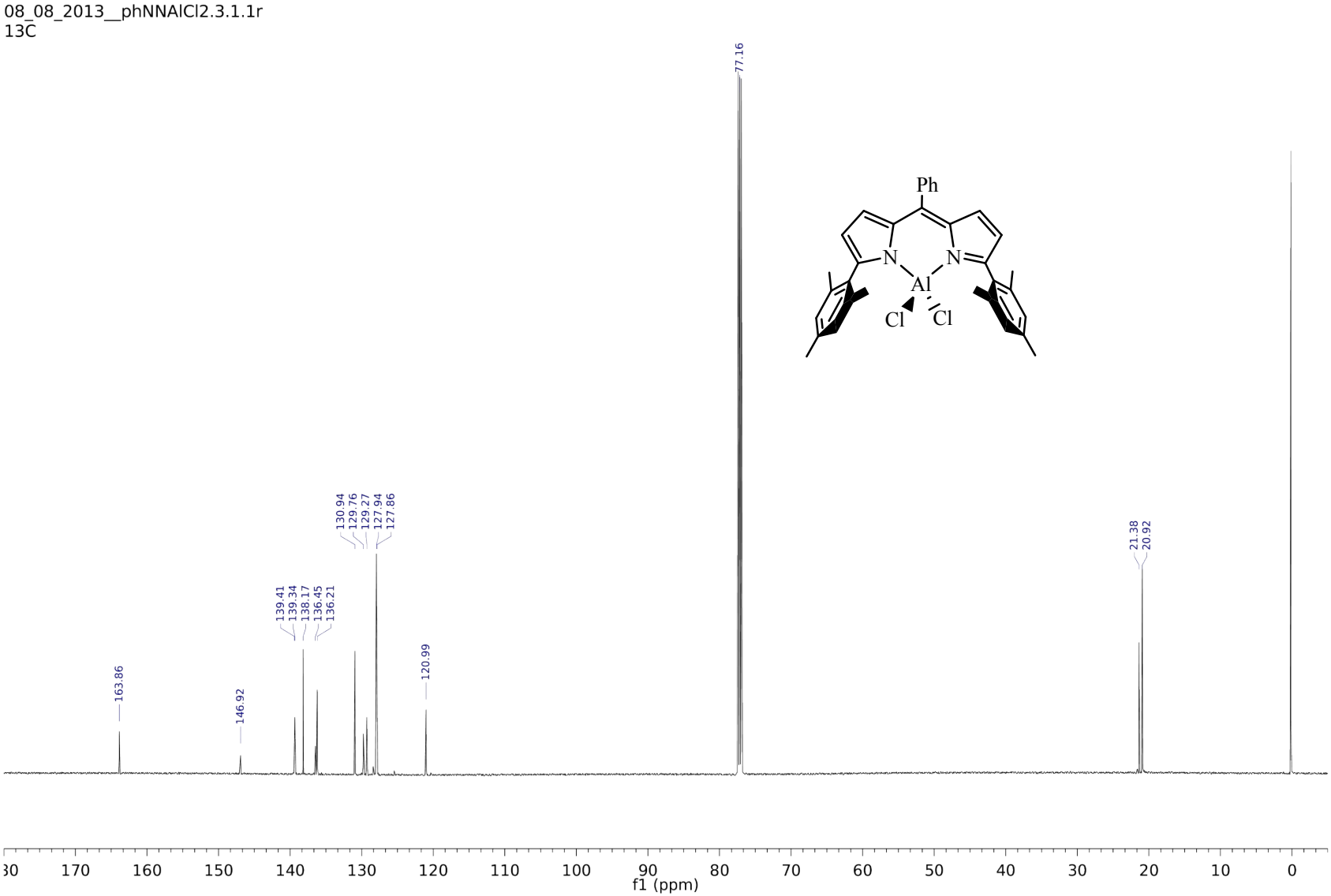

Figure S2. $^{13}C\{^{1}H\}$ NMR spectrum of **2** in $CDCl_3$

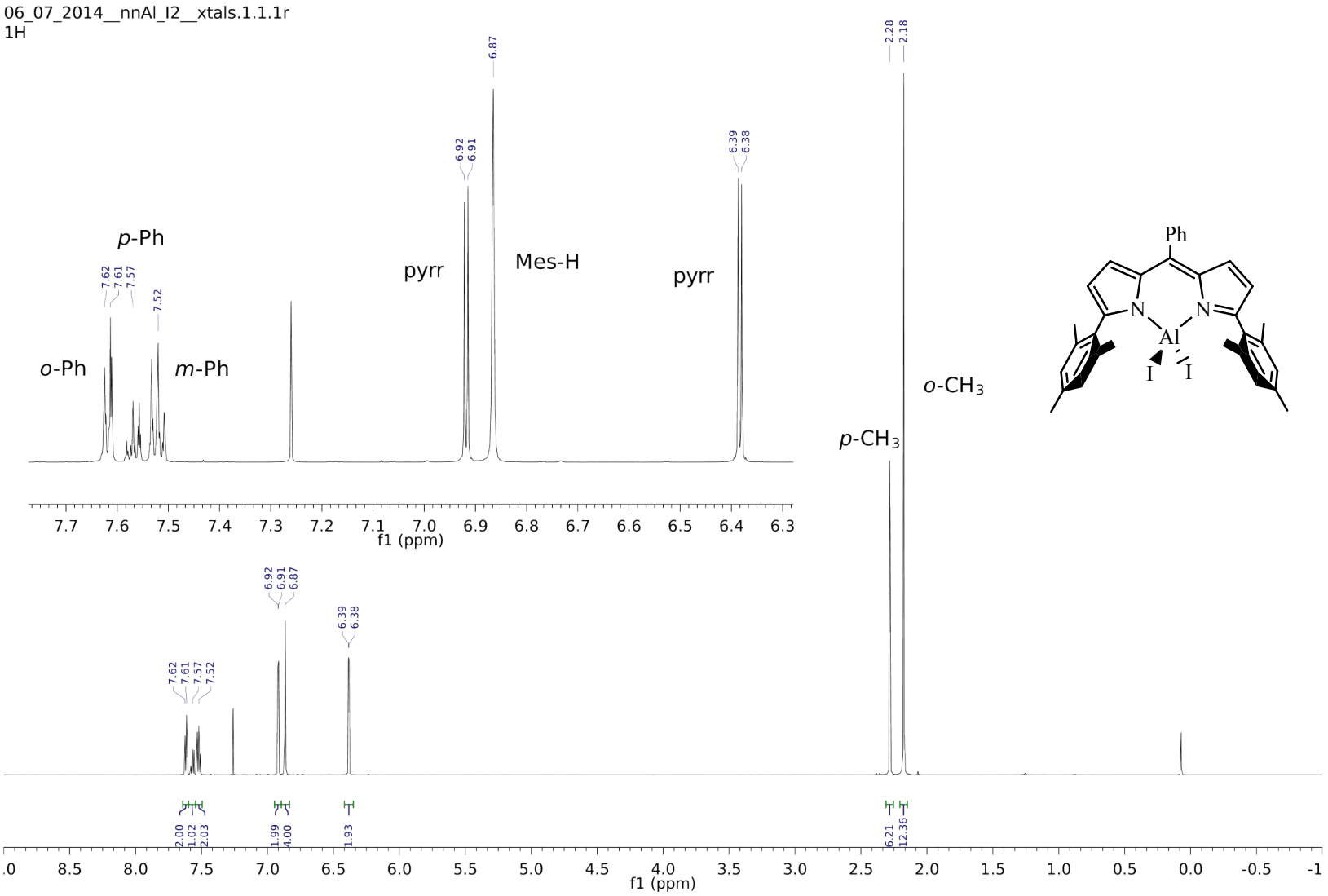

Figure S3. ^{1}H NMR spectrum of **3** in $CDCl_3$

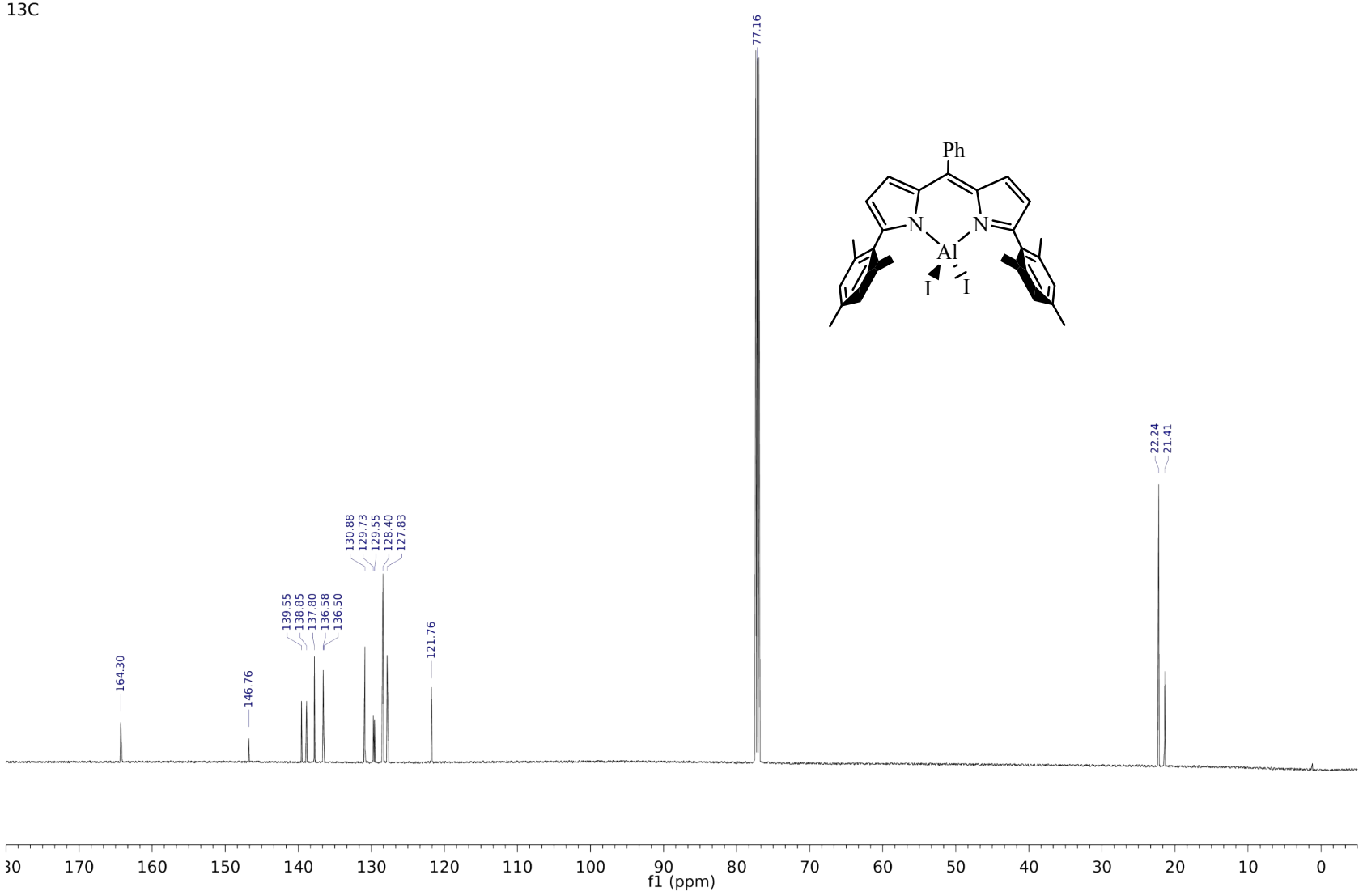

Figure S4. $^{13}C\{^{1}H\}$NMR spectrum of **3** in $CDCl_3$

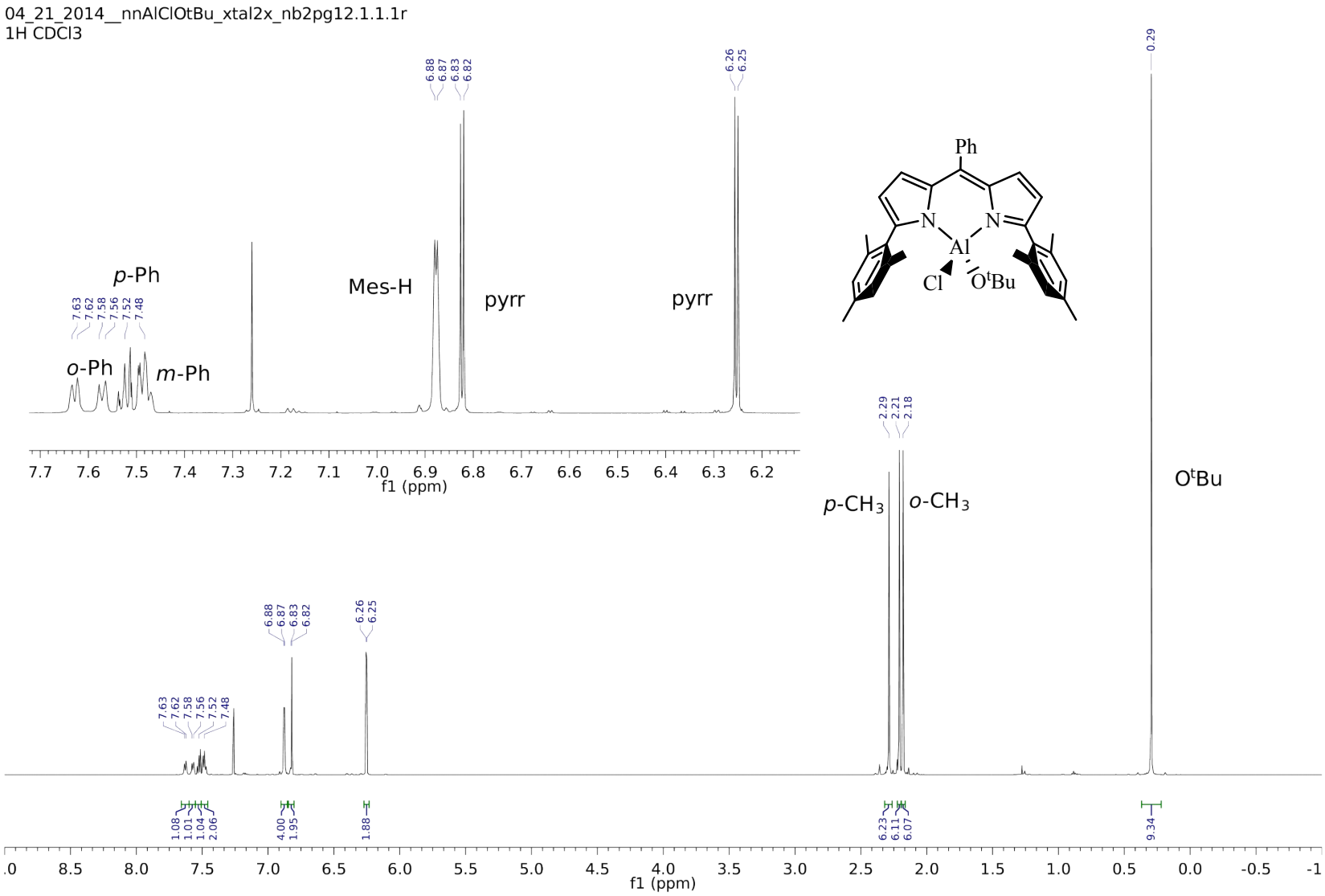

Figure S5. ^{1}H NMR spectrum of **4** in $CDCl_3$

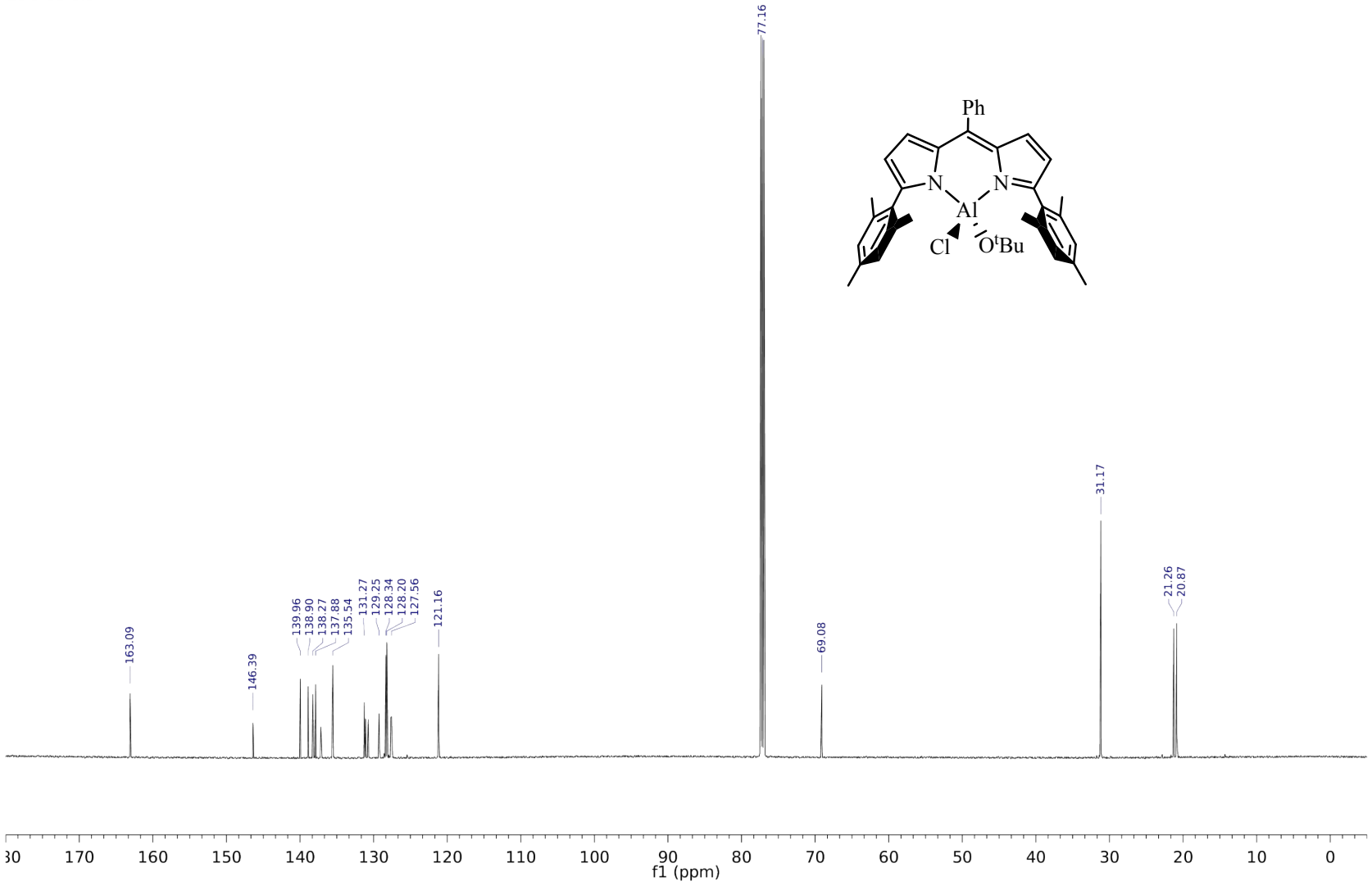

Figure S6. $^{13}C\{^1H\}$NMR spectrum of **4** in $CDCl_3$

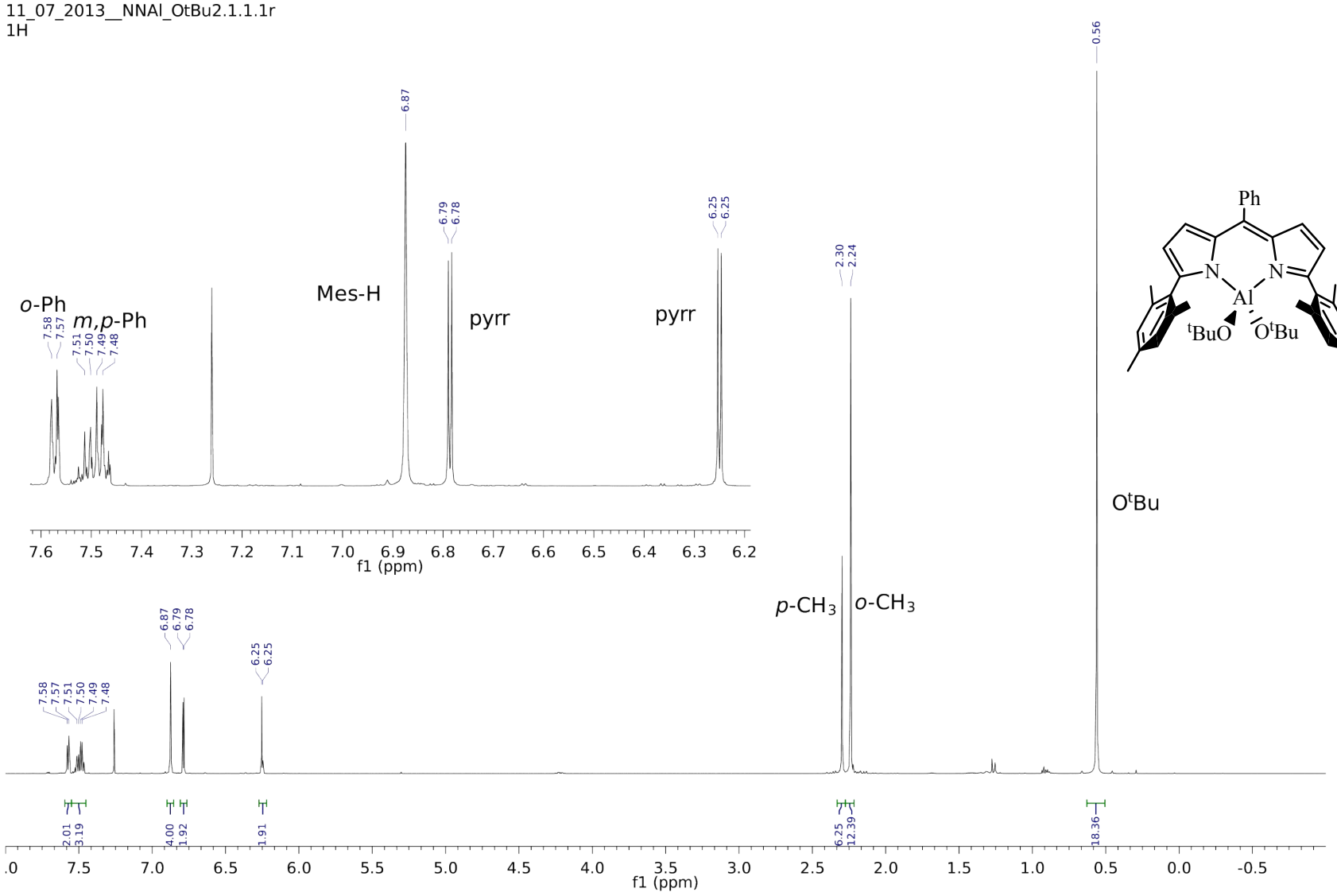

Figure S7. ^{1}H NMR spectrum of **5** in $CDCl_3$

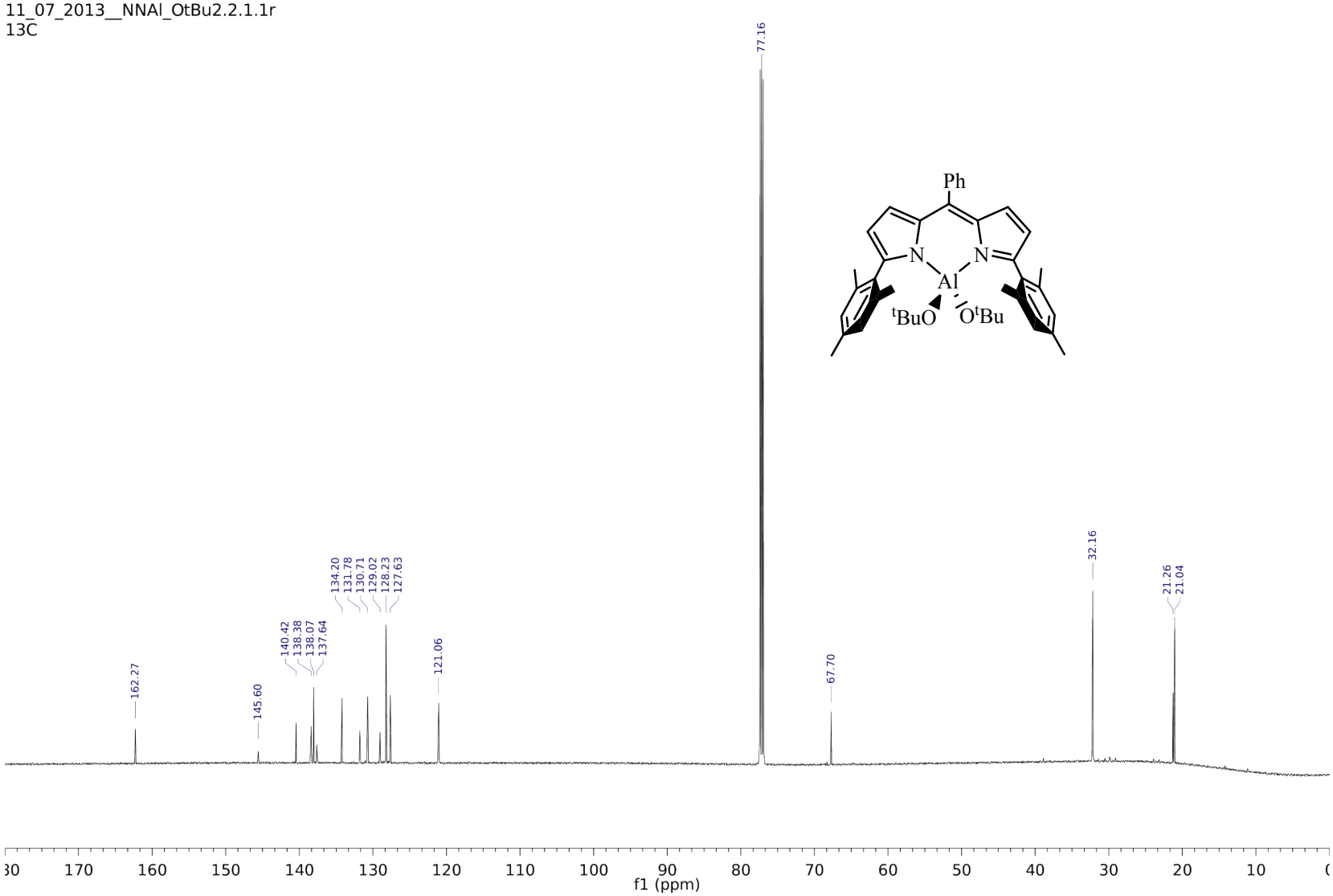

Figure S8. $^{13}C\{^{1}H\}$NMR spectrum of **5** in $CDCl_3$

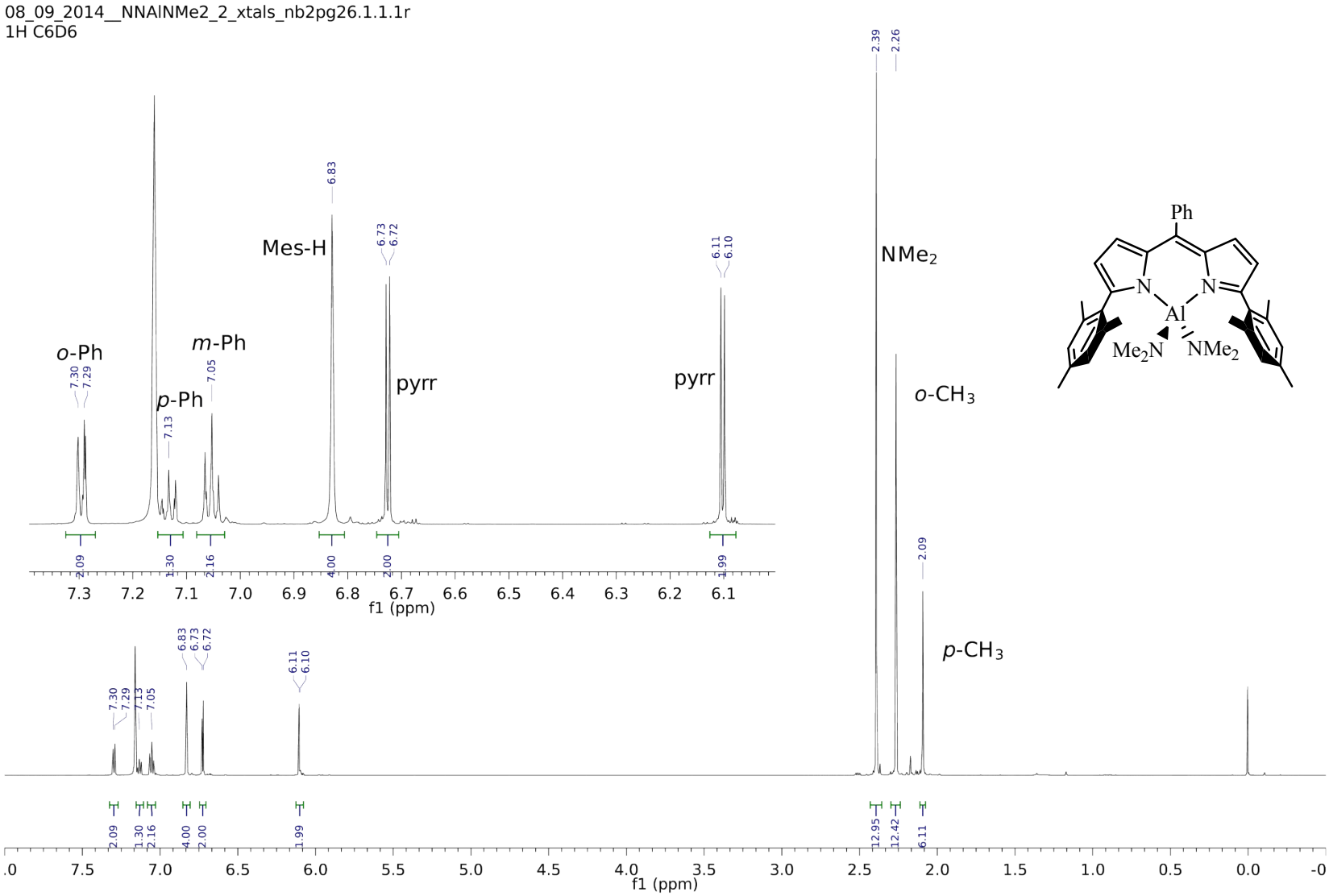

Figure S9. ^{1}H NMR spectrum of **6** in C_6D_6

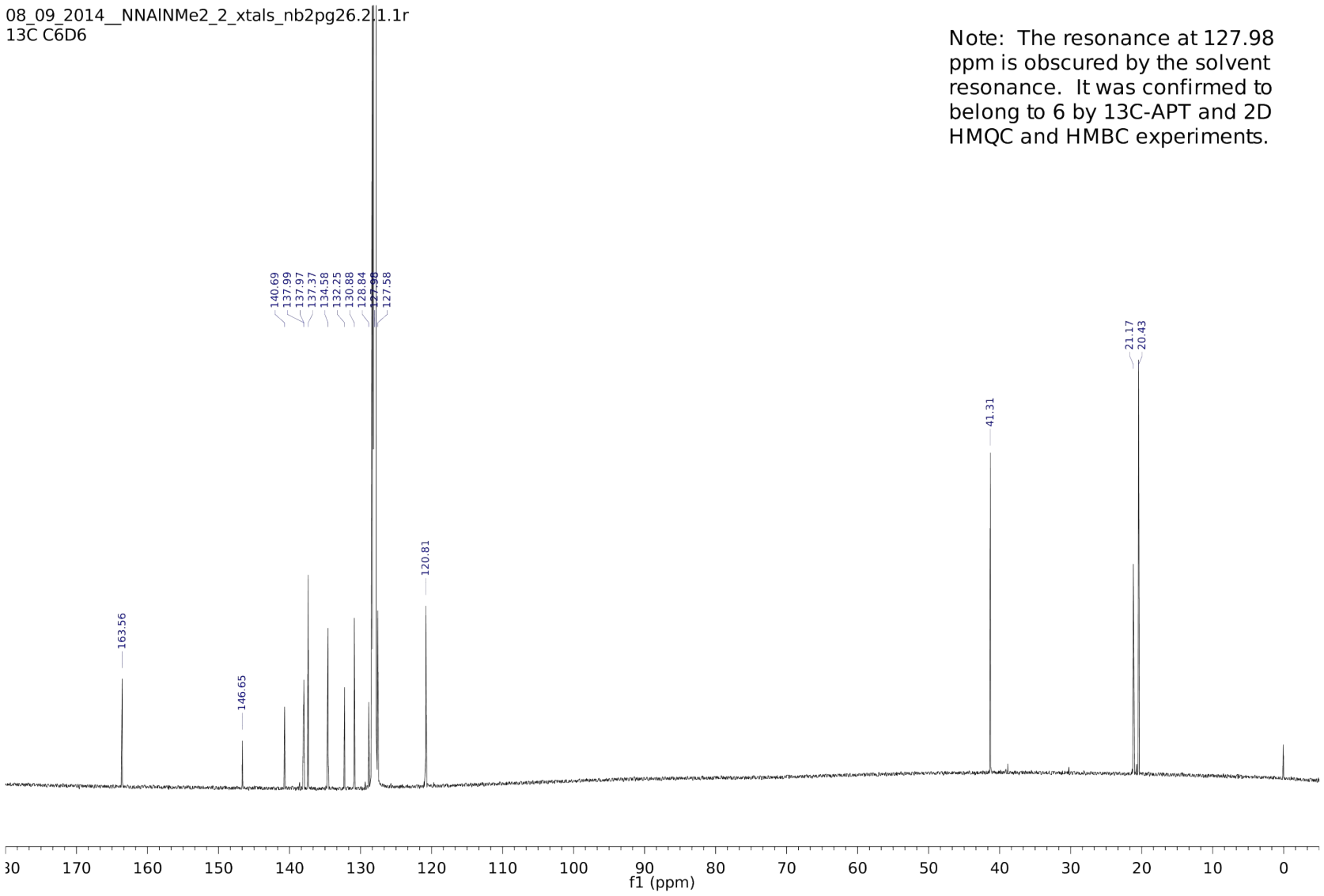

Figure S10. $^{13}C\{^{1}H\}$NMR spectrum of **6** in C_6D_6

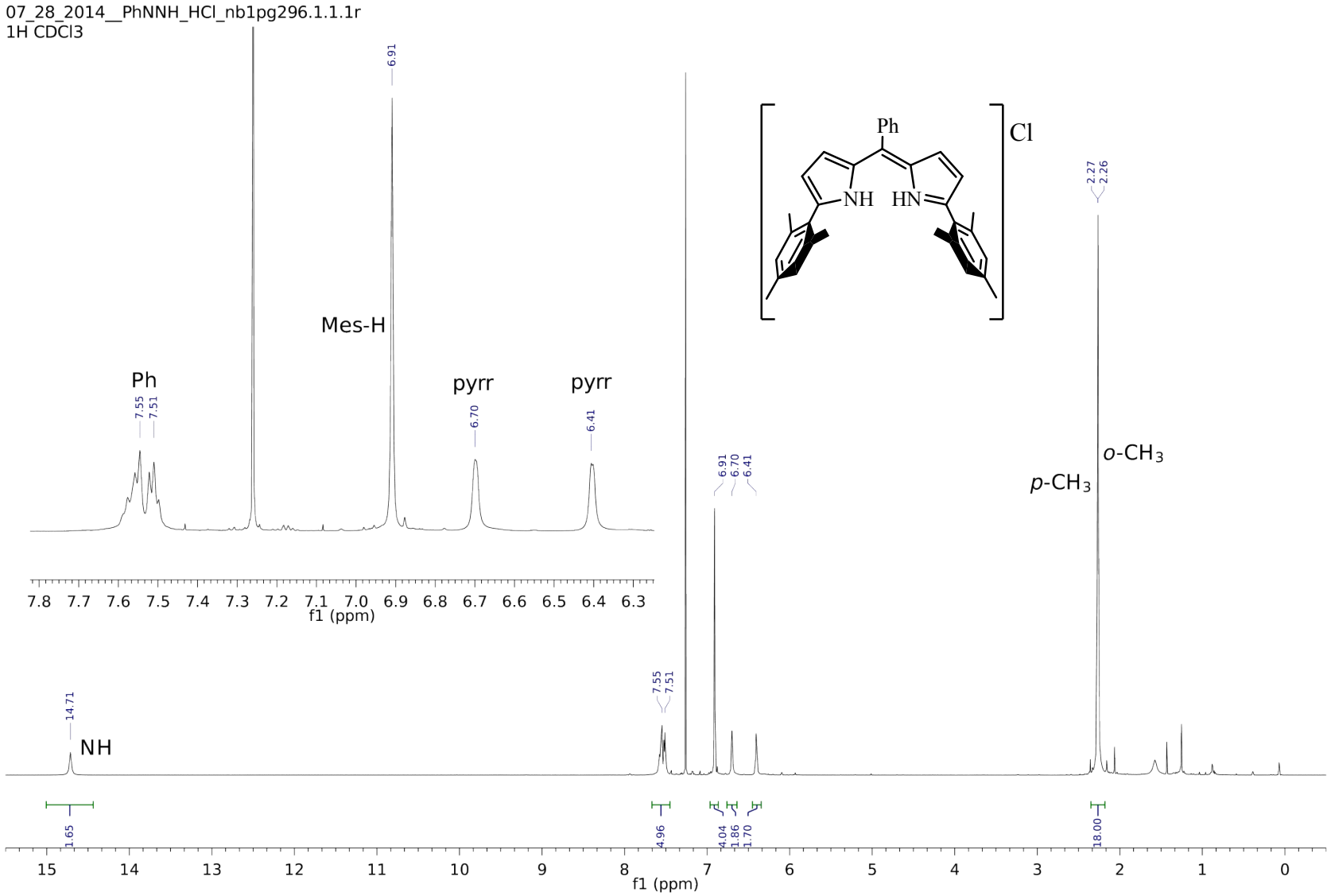

Figure S11. ^{1}H NMR spectrum of **7** in $CDCl_3$

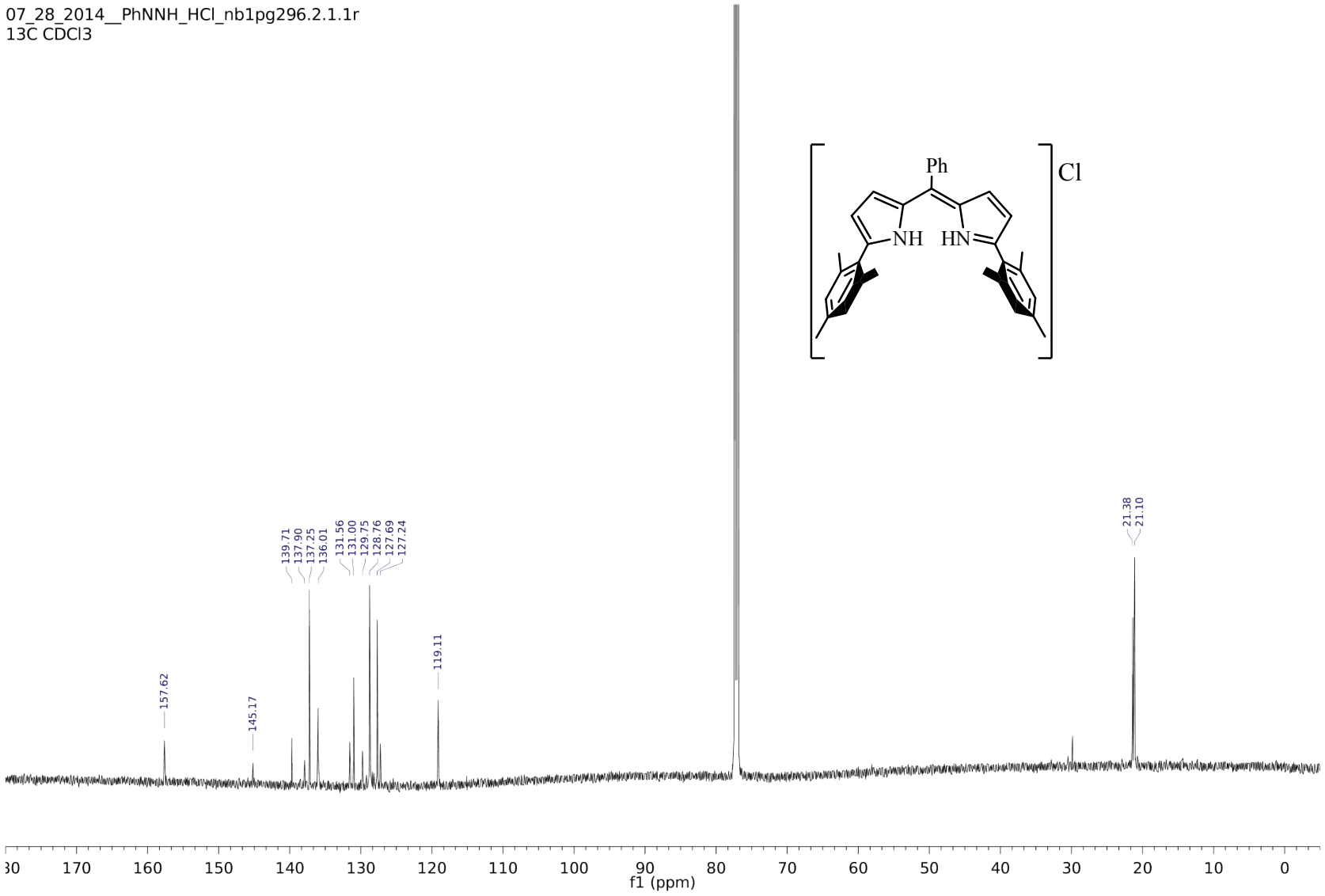

Figure S12. $^{13}C\{^{1}H\}$NMR spectrum of **7** in $CDCl_3$

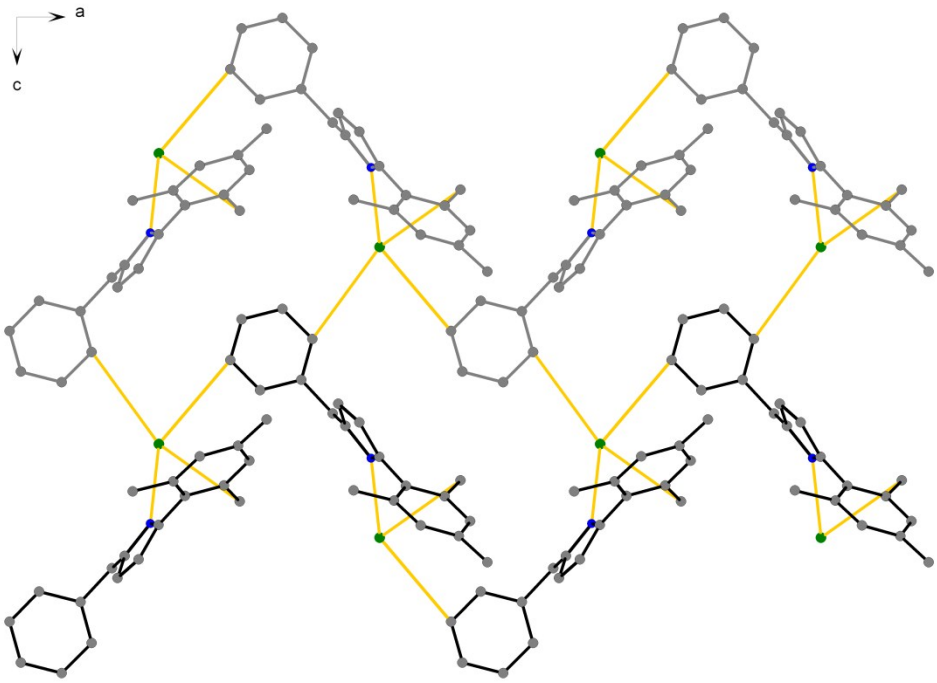

Figure S13. Two-dimensional segment depicting packing in (*N*,*N*)H•HCl (**7**). Two four-molecule saw-tooth arrays are depicted parallel to the crystal *b* axis, one in gray and the other in black. E−H···Cl (E = N, C) interactions are depicted as yellow bonds connecting E hydrogen atoms to chlorine atoms. Carbon atoms are colored gray, nitrogens are colored blue and chlorines are green.

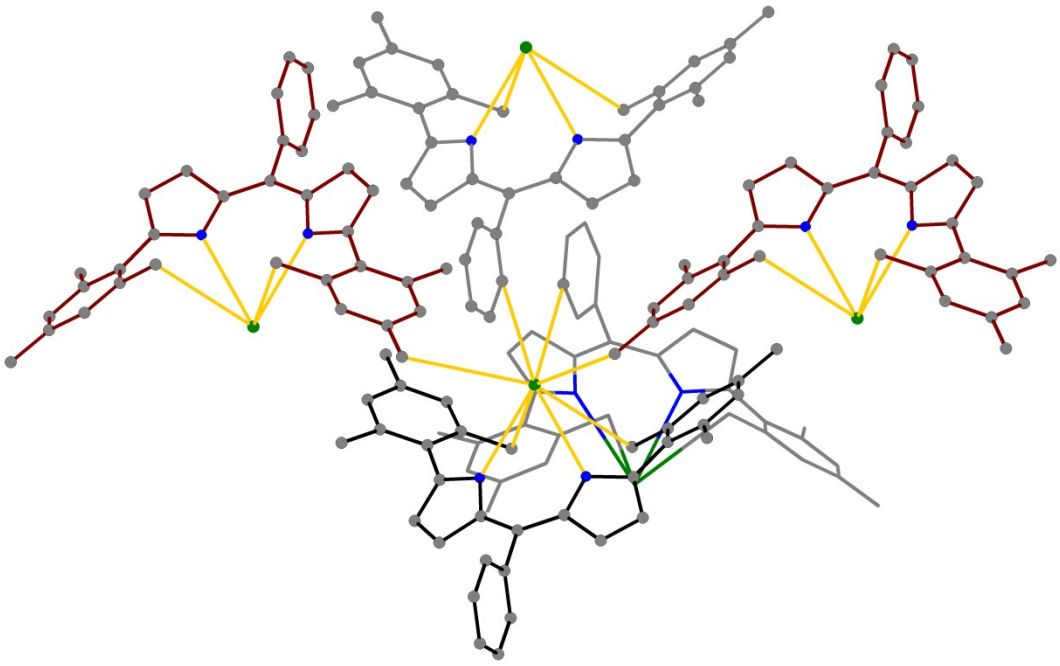

Figure S14. Three-dimensional packing diagram of (*N*,*N*)H•HCl (**7**) showing eight E−H···X interactions (E = N, C). Molecules shown in black and gray belong to the two-dimensional segment as depicted in Figure S13. The molecules in black and in gray wireframe belong to the same 2D segment, while the molecules shown in red are above and below the crystallographic *ac* plane as shown in Figure S13. E−H···X interactions are depicted as yellow bonds connecting E atoms to chlorine atoms. Carbon atoms are colored gray, nitrogen atoms are colored blue and chlorines are green.

Table S1. Crystal Data and Structure Refinement Details

	2	**3**	**4**
formula	$C_{33}H_{31}N_2AlCl_2$	$C_{33}H_{31}N_2AlI_2$	$C_{37}H_{40}AlN_2OCl$
fw	553.48	736.38	591.14
cryst syst	orthorhombic	monoclinic	monoclinic
space group	*Pnn*2	*C*2/*c*	$P2_1/c$
a, Å	10.0003(6)	21.089(4)	15.4551(3)
b, Å	11.7787(7)	13.041(3)	14.5277(3)
c, Å	12.3391(7)	23.489(5)	15.9943(3)
α, deg	90.00	90.00	90.00
β, deg	90.00	104.897(3)	113.696(1)
γ, deg	90.00	90.00	90.00
V, Å^3	1453.4(2)	6243(2)	3288.4(1)
Z	2	8	4
D_{calcd}, g cm^{-3}	1.265	1.567	1.194
T, °C	–123	–133	–153
μ, mm^{-1}	0.278	2.067	1.516
λ, Å	0.71073	0.71073	1.54178
transm coeff	0.719–1.00	0.665-0.746	0.647–0.753
2*θ* limits, deg	4.8–66.6	3.6–56.0	6.2–137.9
total no. of data	47190	146447	27612
no. of unique data	9029	9248	5965
no. of obsd data[a]	8189	8073	5032
no. of params	178	350	544
R_1[b] (F, $I > 2\sigma(I)$)	0.0373	0.0354	0.0427
wR_2[c] (F^2, all data)	0.0890	0.0912	0.1178
max, min peaks, e/Å^3	0.338, –0.182	0.669, –0.603	0.335, –0.404

[a] $I > 2\sigma(I)$. [b] $R_1 = \Sigma \, | \, |F_o| - |F_c| \, | \, / \Sigma \, |F_o|$. [c] $wR_2 = [\Sigma[w \, (F_o^2 - F_c^2)^2] \, / \Sigma[w \, (F_o^2)^2]]^{1/2}$.

Table S1. (continued)

	5	**6**	**7**
formula	$C_{41}H_{49}AlN_2O_2$	$C_{37}H_{43}AlN_4$	$C_{33}H_{33}N_2Cl$
fw	628.80	570.73	493.06
cryst syst	orthorhombic	monoclinic	orthorhombic
space group	$P2_12_12_1$	$P2_1/n$	*Pnma*
a, Å	13.9055(3)	10.159(2)	14.4443(6)
b, Å	15.3152(3)	16.568(3)	18.4741(7)
c, Å	17.3140(4)	19.274(3)	9.5304(3)
α, deg	90.00	90.00	90.00
β, deg	90.00	93.011(3)	90.00
γ, deg	90.00	90.00	90.00
V, Å^3	3687.3(2)	3239.6(9)	2543.1(2)
Z	4	4	4
D_{calcd}, g cm^{-3}	1.133	1.170	1.288
T, °C	–153	–153	–133
μ, mm^{-1}	0.748	0.094	1.506
λ, Å	1.54178	0.71073	1.54178
transm coeff	0.693–0.753	0.700-0.746	0.663-0.753
2*θ* limits, deg	7.7–137.8	3.2–56.0	9.6–133.2
total no. of data	16862	44155	36632
no. of unique data	6728	7830	2263
no. of obsd data[a]	6299	6054	2248
no. of params	460	527	219
R_1[b] (F, $I > 2\sigma(I)$)	0.0331	0.0426	0.0298
wR_2[c] (F^2, all data)	0.0879	0.1161	0.0769
max, min peaks, e/Å^3	0.315, –0.240	0.527, –0.267	0.200, –0.239

[a] $I > 2\sigma(I)$. [b] $R_1 = \Sigma \, | \, |F_o| - |F_c| \, | \, / \Sigma \, |F_o|$. [c] $wR_2 = [\Sigma[w \, (F_o^2 - F_c^2)^2] \, / \Sigma[w \, (F_o^2)^2]]^{1/2}$.

Table S1. (continued)

	8
formula	$C_{33}H_{33}N_2I$
fw	584.51
cryst syst	orthorhombic
space group	*Pnma*
a, Å	14.460(2)
b, Å	18.427(2)
c, Å	10.203(1)
α, deg	90.00
β, deg	90.00
γ, deg	90.00
V, Å^3	2718.5(6)
Z	4
D_{calcd}, g cm^{-3}	1.428
T, °C	–133
μ, mm^{-1}	1.202
λ, Å	0.71073
transm coeff	0.640–0.745
2*θ* limits, deg	4.4–53.5
total no. of data	33730
no. of unique data	3211
no. of obsd data[a]	2649
no. of params	235
R_1[b] (F, $I > 2\sigma(I)$)	0.0320
wR_2[c] (F^2, all data)	0.0866
max, min peaks, e/Å^3	0.573, –0.429

[a] $I > 2\sigma(I)$. [b] $R_1 = \Sigma \, | \, |F_o| - |F_c| \, | \, / \Sigma \, |F_o|$. [c] $wR_2 = [\Sigma[w \, (F_o^2 - F_c^2)^2] \, / \Sigma[w \, (F_o^2)^2]]^{1/2}$.